

1 **Published in Mar Environ Res. (2015) Oct; 111: 34-40. doi: 10.1016/j.marenvres.2015.06.008.**

2

3 **Evidence for immunomodulation and apoptotic processes induced by cationic polystyrene**  
4 **nanoparticles in the hemocytes of the marine bivalve *Mytilus***

5 Canesi L.<sup>1</sup>, Ciacci C.<sup>2</sup>, Bergami E.<sup>3</sup>, Monopoli M. P.<sup>4</sup>, Dawson K. A.<sup>4</sup>, Papa S.<sup>5</sup>, Canonico, B.<sup>2</sup>,  
6 Corsi I.<sup>3</sup>

7 *<sup>1</sup>Dept.of Earth, Environmental and Life Sciences-DISTAV, University of Genoa, Italy; <sup>2</sup>Dept.of*  
8 *Earth, Life and Environmental Sciences-DISTEVA, University of Urbino, Italy; <sup>3</sup>Dept. of Physical,*  
9 *Earth and Environmental Sciences, University of Siena, Italy; <sup>4</sup>Centre for BioNanoInteractions,*  
10 *School of Chemistry and Chemical Biology, University College Dublin, Ireland; <sup>5</sup>Department of*  
11 *Biomolecular Sciences-DISB, University of Urbino, Italy.*

12

13

14

15 \* Address correspondence to [Laura.Canesi@unige.it](mailto:Laura.Canesi@unige.it)

16 DISTAV-Dipartimento di Scienze della Terra, dell'Ambiente e della Vita,  
17 Università di Genova

18 Corso Europa 26

19 16132-Genova

20 Italy

21 Tel: +390103538259

22 Fax:+390103538267

23 [Laura.Canesi@unige.it](mailto:Laura.Canesi@unige.it)

24

25

26 Key words: nanoplastics, marine invertebrates, immunity, apoptosis

27

28  
29  
30  
31  
32  
33  
34  
35  
36  
37  
38  
39  
40  
41  
42  
43  
44  
45  
46  
47  
48  
49  
50  
51  
52  
53

## Abstract

Polymeric nanoparticles can reach the marine environment from different sources as weathering of plastic debris and nanowaste. Nevertheless, few data are available on their fate and impact on marine biota. Polystyrene nanoparticles (PS NPs) can be considered as a model for studying the effects of nanoplastics in marine organisms: recent data on amino-modified PS NPs (PS-NH<sub>2</sub>) toxicity in sea urchin embryos underlined that marine invertebrates can be biological targets of nanoplastics. Cationic PS NPs have been shown to be toxic to mammalian cells, where they can induce apoptotic processes; however, no information is available on their effects and mechanisms of action in the cells of marine organisms. In this work, the effects of 50 nm PS-NH<sub>2</sub> were investigated in the hemocytes of the marine bivalve *Mytilus galloprovincialis*. Hemocytes were exposed to different concentrations (1, 5, 50 µg/ml) of PS-NH<sub>2</sub> suspension in ASW. Clear signs of cytotoxicity were evident only at the highest concentrations (50 µg/ml). On the other hand, a dose dependent decrease in phagocytic activity and increase in lysozyme activity were observed. PS-NH<sub>2</sub> NPs also stimulated increase in extracellular ROS (reactive oxygen species) and NO (nitric oxide) production, with maximal effects at lower concentrations. Moreover, at the highest concentration tested, PS-NH<sub>2</sub> NPs induced apoptotic process, as evaluated by Flow cytometry (Annexin V binding and mitochondrial parameters). The results demonstrate that in marine invertebrates the immune function can represent a significant target for PS-NPs. Moreover, in *Mytilus* hemocytes, PS-NH<sub>2</sub> NPs can act through mechanisms similar to those observed in mammalian cells. Further research is necessary on specific mechanisms of toxicity and cellular uptake of nanoplastics in order to assess their impact on marine biota.

## 54 1. Introduction

55

56 Plastic debris and their degradation products into smaller fragments, at the micro-, and  
57 potentially also the nano-scale level, as well as microplastics present in different items, such as  
58 cosmetics, are widespread in the marine environment, both in oceans and sediments (Cole et al.,  
59 2011; Hidalgo-Ruz et al., 2012; Wright et al., 2013). Occurrence of nanoplastics in the sea and their  
60 possible impact on marine organisms is obviously part of the growing concern for the continuous  
61 and increasing release of plastic wastes in the aquatic compartment, including estuarine and coastal  
62 areas (Wegner et al., 2012; Corsi et al., 2014). In general, bioavailability of micro- and nano-  
63 plastics may depend on their size, density, shape, and surface charges which will affect their  
64 behaviour in sea water, leading to agglomeration, resuspension and settling; moreover, their uptake,  
65 disposal and bioaccumulation by marine organisms is influenced by their feeding behaviour, with  
66 benthic detritivores and suspension feeders representing more susceptible target species (Wright et  
67 al., 2013). Microplastics have been detected in edible marine bivalves, indicating also a possible  
68 threat to seafood safety (Van Cauwenberghe and Janssen, 2014).

69 Polystyrene (PS) is one of the most largely used plastics worldwide, used in food and industrial  
70 packaging, disposable cutlery, compact disc cases, building insulation, medical products and toys  
71 (Andrady 2011; Plastic Europe, 2013). This versatile and non-biodegradable polymer is found in  
72 the oceans as micro- and nano-debris, accounting for 24% of the macroplastics in the estuarine  
73 habitat (Browne et al., 2008). One of the first evidences of PS impact on filter-feeders is reported by  
74 Ward et al. (2009), showing that marine aggregates of nano-sized PS facilitate food ingestion and  
75 are translocated from the gut to the circulatory system, where they are retained for more than a  
76 month (Ward et al., 2009). Concerning nano-scale PS, only few studies have so far investigated the  
77 possible effects in marine species. In the blue mussel *M. edulis*, feeding rate was affected and an  
78 increased production of pseudofaeces was observed (Wegner et al., 2012). In our previous study,  
79 with sea urchin embryo (*P. lividus*), exposure to PS NPs, in particular amino-modified PS NPs (PS-  
80 NH<sub>2</sub>) caused severe developmental defects (with an EC<sub>50</sub> of 3.85 µg/mL) and induced *cas8* gene  
81 expression at 24 h post fertilization, suggesting the involvement of apoptotic pathways (Della Torre  
82 et al., 2014). However, no information is yet available on the effects of PS NPs at cellular level in  
83 marine organisms. The importance of the immune system as a target of NPs toxicity has been  
84 already described in two model marine organisms, the bivalve *Mytilus* spp. and the sea urchin  
85 *Paracentrotus lividus* (Canesi et al., 2012; Matranga and Corsi, 2012; Canesi and Procházková,  
86 2013; Corsi et al., 2014). These studies underlined that NPs affect lysosomal function, stimulate the  
87 production of reactive oxygen species, and decrease the phagocytic activity in *Mytilus* immune  
88 cells, the hemocytes (reviewed in Canesi and Procházková, 2013).

89 PS NPs are well established in a variety of biological and medical applications including fast  
90 synthesis, low costs, easy separation and surface modification. The importance of particle surface  
91 functionalization for targeted biomedical application, as well as particle charge as potential  
92 determinant factor of cytotoxicity has been underlined in a number of studies on the interactions  
93 between functionalized cationic and anionic PS NPs and mammalian cells (Fleischer and Payne,  
94 2014). In particular, cationic particles, such as PS-NH<sub>2</sub>, have shown more adverse effects than  
95 anionic particles (Liu et al., 2011). A cationic surface would enable the particle to interact with the  
96 cell membrane more easily due to their similar molecular structure to proteins, hence, promoting the  
97 cell uptake of the NPs (Nel et al., 2009). For example, in human macrophages, PS-NH<sub>2</sub> trigger

98 inflammasome activation and subsequent release of proinflammatory cytokines, induce lysosomal  
99 membrane destabilization and release of lysosomal enzymes, as well as production of reactive  
100 oxygen species (Lunov et al., 2011). In human astrocytoma cells, PS-NH<sub>2</sub> also induced lysosomal  
101 damage and apoptotic processes (Bexiga et al, 2011; Wang et al., 2013). In mammalian cells,  
102 different NPs, including PS-NH<sub>2</sub> associate with serum soluble components, organized into a  
103 “protein corona”, which affects particle interactions (internalization and effects) (Fleischer and  
104 Payne, 2014 and refs. quoted therein). However, no information is available on the interactions of  
105 functionalized PS NPs in the cells of marine organisms.

106 In this work, a battery of functional immune assays was applied to investigate the short term *in*  
107 *vitro* effects of PS NPs on *Mytilus* immune cells. For this first study, PS-NH<sub>2</sub> were chosen as a  
108 model of functionalized PS NPs on the basis of their stronger toxicity demonstrated in both in both  
109 mammalian cells and the sea urchin. Several functional parameters were evaluated: lysosomal  
110 membrane stability and lysosomal enzyme release, extracellular oxyradical production and Nitric  
111 Oxide (NO) production, phagocytic activity, as well as pro-apoptotic processes at both plasma  
112 membrane and mitochondrial level.

113

114

## 115 **2. Materials and methods**

116

### 117 *2.1 Characterization of PS-NH<sub>2</sub> nanoparticles*

118 Primary characterization of unlabelled 50 nm amino polystyrene NPs (PS-NH<sub>2</sub>), purchased  
119 from Bangs Laboratories, was performed as described in our previous paper (Della Torre et al.,  
120 2014). Primary particle diameter of PS-NH<sub>2</sub> was determined by transmission electron microscopy  
121 (Philips Morgagni 268D electronics, at 80 KV and equipped with a MegaView II CCd camera.  
122 Artificial sea water (ASW) was prepared according to ASTM protocol (pH 8, salinity 36 ‰)  
123 (ASTM 2004) and filtered with 0.22 µm membrane. PS-NH<sub>2</sub> suspensions (50 µg/ml) were prepared  
124 in ASW, quickly vortexed prior to use but not sonicated. Size (Z-average and polydispersity index,  
125 PDI) and zeta potential (ζ-potential, mV) were determined by Dynamic Light Scattering (Malvern  
126 instruments), using a Zetasizer Nano Series software, version 7.02 (Particular Sciences, UK).  
127 Measurements were performed in triplicate, each containing 11 runs of 10 seconds for determining  
128 Z-average, 20 runs for the ζ-potential.

129

### 130 *2.2 Animals, hemolymph collection, preparation of hemocyte monolayers and hemocyte treatment*

131 Mussels (*Mytilus galloprovincialis* Lam.) 4–5 cm long, sampled from an unpolluted area at  
132 Cattolica (RN) were obtained from SEA (Gabicce Mare, PU) and kept for 1–3 days in static tanks  
133 containing artificial sea water (ASW) (1 l/mussel) at 16°C. Sea water was changed daily.  
134 Hemolymph was extracted from the posterior adductor muscle of 8–20 mussels, using a sterile 1 ml  
135 syringe with a 18 G1/2” needle. With the needle removed, hemolymph was filtered through a sterile  
136 gauze and pooled in 50 ml Falcon tubes at 4°C. Hemocyte monolayers were prepared as previously  
137 described (Canesi et al., 2008). Hemocytes were incubated at 16°C with different concentrations of  
138 PS-NH<sub>2</sub> in ASW, unless otherwise indicated, for different periods of time, depending on the time of  
139 endpoint measured. Short-term exposure conditions (from 30 min to 4 hrs) were chosen to evaluate  
140 the rapid *in vitro* responses to PS-NH<sub>2</sub> at concentrations of 1, 5 and 50 µg/ml (corresponding to 1.46  
141 x 10<sup>10</sup>, 7.31 x 10<sup>10</sup>, and 7.31 x 10<sup>11</sup> particles/ml, respectively), in analogy with those previously

142 observed with other types of NPs in mussel hemocytes (Canesi et al., 2008; Canesi et al., 2010;  
143 Ciacci et al., 2012) and with studies carried out with functionalized PS NPs in human cells (Lunov  
144 et al., 2011; Wang et al., 2013). Untreated (control in ASW) hemocyte samples were run in parallel.  
145

### 146 2.3 Hemocyte functional assays

147 Hemocyte functional parameters (lysosomal membrane stability, lysosomal enzyme release,  
148 phagocytosis, extracellular oxyradical production, Nitric oxide production) were evaluated  
149 essentially as previously described (Canesi et al., 2008; Canesi et al., 2010; Ciacci et al., 2012).  
150 Lysosomal membrane stability in control hemocytes and hemocytes pre-incubated with different  
151 concentrations of PS-NH<sub>2</sub> (1, 5, 50 µg/ml) for 30 min was evaluated by the Neutral Red Retention  
152 time assay. Hemocyte monolayers on glass slides were incubated with 30 µl of a NR solution (final  
153 concentration 40 µg/ml from a stock solution of NR 40 mg/ml DMSO); after 15 min excess dye was  
154 washed out, 30 µl of ASW, and slides were sealed with a coverslip. Control hemocytes were run in  
155 parallel. Every 15 min slides were examined under an optical microscope and the percentage of  
156 cells showing loss of the dye from lysosomes in each field was evaluated. For each time point 10  
157 fields were randomly observed, each containing 8-10 cells. The endpoint of the assay was defined  
158 as the time at which 50% of the cells showed sign of lysosomal leaking (the cytosol becoming red  
159 and the cells rounded). For each experiment, control hemocyte samples were run in parallel.  
160 Triplicate preparations were made for each sample. All incubations were carried out at 16°C.

161 Lysosomal enzyme release was evaluated by measuring lysozyme activity in the extracellular  
162 medium. To obtain hemolymph serum (i.e., hemolymph free of cells), whole hemolymph was  
163 centrifuged at 200 x g for 10 min, and the supernatant was passed through a 0.22 µm filter. Briefly,  
164 lysozyme activity in aliquots of serum of hemocytes incubated with or without PS-NH<sub>2</sub> for different  
165 periods of time (from 30 to 60 min) was determined spectrophotometrically at 450 nm utilizing  
166 *Micrococcus lysodeikticus*.

167 Phagocytosis Assay: phagocytosis of neutral red-stained zymosan by hemocyte monolayers  
168 was used to assess the phagocytic ability of hemocytes. Neutral red-stained zymosan in 0.05 M  
169 Tris-HCl buffer (TBS), pH 7.8, containing 2% NaCl was added to each monolayer at a  
170 concentration of about 1:30 hemocytes:zymosan in the presence or absence of PS-NH<sub>2</sub> (1, 5 and 50  
171 µg/ml), and allowed to incubate for 60 min. Monolayers were then washed three times with TBS,  
172 fixed with Baker's formol calcium (4%, v/v, formaldehyde, 2% NaCl, 1% calcium acetate) for 30  
173 min and mounted in Kaiser's medium for microscopical examination with a Vanox optical  
174 microscope. For each slide, the percentage of phagocytic hemocytes was calculated from a  
175 minimum of 200 cells.

176 Extracellular generation of superoxide was measured by the reduction of cytochrome c.  
177 Hemolymph was extracted into an equal volume of TBS (0.05M Tris-HCl buffer, pH 7.6,  
178 containing 2% NaCl). Aliquots (500 µl) of hemocyte suspension in triplicate were incubated with  
179 500 µl of cytochrome c solution (75 µM ferricytochrome c in TBS), with or without PS-NH<sub>2</sub> (final  
180 concentration 1, 5, 50 µg/ml). Cytochrome c in TBS was used as a blank. Samples were read at 550  
181 nm at different times (from 0 to 30 min) and the results expressed as changes in OD per mg protein.

182 Nitric oxide (NO) production by mussel hemocytes was evaluated as described previously by  
183 the Griess reaction, which quantifies the nitrite (NO<sub>2</sub><sup>-</sup>) content of supernatants. Aliquots of  
184 hemocyte suspensions (1.5 ml) were incubated at 16°C with 1, 5, 10 µg/ml of PS-NH<sub>2</sub> for 0-4 h.  
185 Every 60 min, samples were immediately frozen and stored at -80°C until use. Before analysis,

186 samples were thawed and centrifuged (12,000 x g for 30 min at 4°C), and the supernatants were  
187 analyzed for NO<sub>2</sub><sup>-</sup> content. Aliquots (200 µl) in triplicate were incubated for 10 min in the dark with  
188 200 µl of 1% (wt/v) sulphanilamide in 5% H<sub>3</sub>PO<sub>4</sub> and 200 µl of 0.1% (wt/v) N-(1-naphthyl)-  
189 ethylenediamine dihydrochloride. Samples were read at 540 nm, and the molar concentration of  
190 NO<sub>2</sub><sup>-</sup> in the sample was calculated from standard curves generated using known concentrations of  
191 sodium nitrite.

192 Finally, the possible effect of hemolymph serum on PS-NH<sub>2</sub>-induced lysosomal membrane  
193 destabilization were also evaluated. Hemocytes were incubated for 30 min with PS-NH<sub>2</sub> suspensions  
194 (1, 5, 50 µg/ml) in filtered hemolymph serum and LMS was evaluated as described above. The results  
195 were compared with those obtained in ASW.

196

#### 197 2.4 Flow cytometry (FC)

198 Aliquots of hemolymph were incubated with PS-NH<sub>2</sub> (final concentration 1, 5, 50 µg/ml) for  
199 45 min at 18°C and analyzed on a FACSCalibur flow cytometer (Becton Dickinson, San Diego,  
200 CA, USA). Samples (each containing about 1-2·10<sup>6</sup> cells/mL) were then stained with different  
201 fluorescent probes for FC analysis. All incubations were carried out at 18°C.

202 Annexin V-FITC and propidium iodide (PI) test was carried out as previously described (Ciacci  
203 et al., 2012): aliquots of 1 ml hemolymph were pelleted by centrifugation (100 x g for 10 min) and  
204 resuspended in 300 µl of annexin-binding buffer (10 mM Hepes and 3.3 mM CaCl<sub>2</sub>, pH 7.4)  
205 adjusted for salinity by addition of 2% NaCl. FITC-Annexin V (Bender MedSystem, Vienna,  
206 Austria) then PI (Sigma) was added to final concentration of 1 mg/ml. Cells were incubated for 15  
207 min in the dark at 16°C and then processed for FC analyses. For each experimental condition,  
208 10.000 events were collected. Annexin V FITC and PI fluorescence were collected on the  
209 logarithmic scale for all experiments.

210 Mitochondrial parameters were evaluated as previously described (Ciacci et al., 2012). The  
211 effects of PS-NH<sub>2</sub> on mitochondrial membrane potential (MMP, Δψ<sub>m</sub>) were evaluated by the  
212 fluorescent dye Tetramethylrhodamine, ethyl ester perchlorate (TMRE). TMRE is a quantitative  
213 marker for the maintenance of the mitochondrial membrane potential and it is accumulated within  
214 the mitochondrial matrix in accordance to the Nernst equation. TMRE exclusively stains the  
215 mitochondria and is not retained in cells upon collapse of the Δψ<sub>m</sub>, which is an early step of  
216 apoptotic processes. Hemocytes were incubated with 40 nM TMRE for 10 min before FC analysis  
217 using an excitation wavelength of 488 nm and an emission wavelength of 580 nm. Mitochondrial  
218 cardiolipin (CL) peroxidation was also evaluated by the CL sensitive probe, 10-nonyl-acridine  
219 orange (NAO). After exposure to PS-NH<sub>2</sub>, cells were collected by centrifugation, washed in PBS-  
220 NaCl buffer, resuspended in the same buffer containing 100 nM NAO and incubated for 30 min. To  
221 evaluate changes in fluorescence intensity (FI) values of TMRE and NAO induced by PS-NH<sub>2</sub>, we  
222 considered the original input on untreated cells as control (100%) (Ciacci et al., 2012).

223 Sample acquisition and analyses were performed by means of a FACSCalibur flow cytometer  
224 equipped with CellQuest<sup>TM</sup> software and data were expressed as mean±SD of at least three  
225 experiments.

#### 226 2.5 Confocal microscopy

227 Cells were exposed to PS-NH<sub>2</sub> (50 and 100 µg/ml) and loaded with TMRE and NAO as  
228 described above. Aliquots of samples analysed by flow cytometry were seeded on glass bottom  
229 culture dishes; fluorescence of TMRE (excitation 568 nm, emission 590–630 nm), and NAO

230 (excitation 488 nm, emission 490–550 nm) was detected using a Leica TCS SP5 confocal setup  
231 mounted on a Leica DMI 6000 CS inverted microscope (Leica Microsystems, Heidelberg,  
232 Germany) using 63x 1.4 oil objective (HCX PL APO 63.0 x 1.40 OIL UV). Images were analyzed  
233 by the Leica Application Suite Advanced Fluorescence (LASAF) and ImageJ Software (Wayne  
234 Rasband, Bethesda, MA).

235

## 236 2.6 Statistics

237 Data are the mean  $\pm$  SD of at least 3 independent experiments in triplicate. Statistical analysis  
238 was performed by using ANOVA plus Tukey's post hoc test.

239

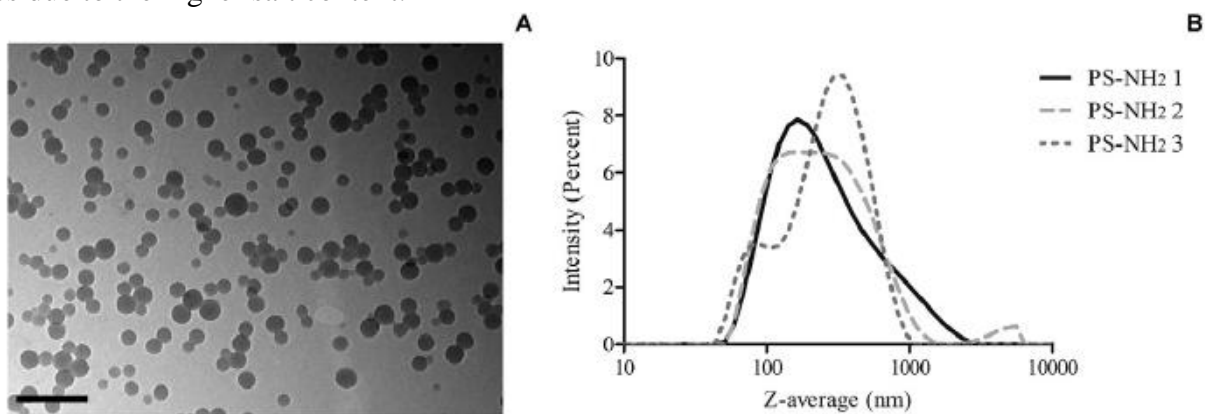
240

## 241 3. Results

242

### 243 3.1 Particle characterization

244 In Fig. 1 and Tab. 1 are reported data on characterization of primary PS-NH<sub>2</sub> particles and of  
245 particle suspension in ASW. TEM analysis (Fig. 1A) of PS-NH<sub>2</sub> confirmed their nominal size of 50  
246 nm reported by Della Torre et al. (2014). DLS analysis of PS-NH<sub>2</sub> suspensions in ASW (50  $\mu$ g/ml)  
247 revealed the formation of small aggregates with a Z-average of 200.3 nm, a PDI of 0.302 and a  $\zeta$ -  
248 potential of +14.2 mV (Fig. 1B and Tab. 1). Behaviour of PS-NH<sub>2</sub> in ASW was similar to that  
249 previously observed in natural sea water (NSW) (Della Torre et al., 2014); in contrast, when  
250 particles were suspended in MilliQ water, no agglomeration occurred and a higher  $\zeta$ -potential was  
251 observed ( $+43 \pm 1$  mV) (Tab. 1). Lower absolute values of  $\zeta$  potential observed in both ASW and  
252 NSW (as compared to those measured in MilliQ water, suggest a screening effect of surface  
253 charges due to the higher salt content.



254

255 Fig. 1. Primary and secondary characterization of PS-NH<sub>2</sub> using TEM imaging and DLS, respectively. Left: TEM  
256 image of primary 50 nm PS-NH<sub>2</sub>. Scale bar: 200 nm. Right: Size

257 distribution graph by intensity for PS-NH<sub>2</sub> suspension at 50 mg/ml in ASW, determined by Contin analysis (DLS  
258 Analysis). Three independent replicates are shown, the x-axis minimum set at 10 nm and a logarithmic scale is used for  
259 y-axis. The graph was edited using GraphPad Prism5.

260

261

**Table 1**

Physico-chemical characterization of PS-NH<sub>2</sub> in Milli-Q water and artificial sea water (ASW) (0.22 μm filtered, T = 18 °C, salinity 36‰, pH 8) using DLS analysis showing Z-average (nm), polydispersity index (PDI) and ζ-potential (mV). Data are referred to PS-NH<sub>2</sub> concentration of 50 μg/ml and values reported as mean ± standard deviation.

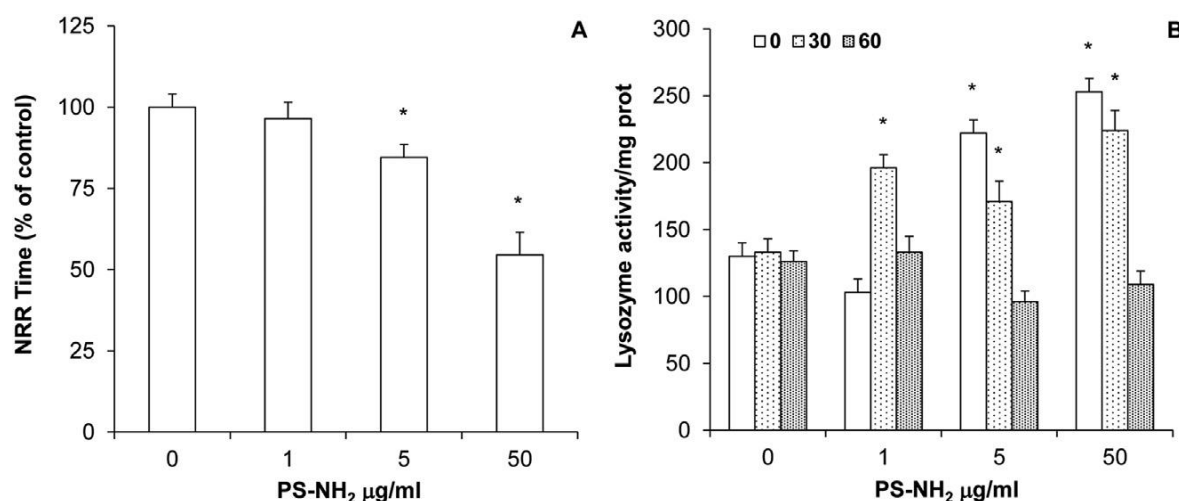
	50 nm PS-NH <sub>2</sub>		
	Z-Average (nm)	PDI	ζ-potential (mV)
MilliQ	57 ± 2	0.07 ± 0.02	+43 ± 1
ASW	200 ± 6	0.302 ± 0.02	+14 ± 2

262  
263

### 264 3.2 Effects of PS-NH<sub>2</sub> on hemocyte functional parameters

265 The effects of PS-NH<sub>2</sub> on *Mytilus* hemocytes were evaluated using a battery of assays, utilizing  
266 different exposure times (from 30 min to 4 h) and conditions optimized for each assay as previously  
267 described (Ciacci et al., 2012). Lysosomal membrane stability (LMS) and lysozyme release were  
268 evaluated in hemocytes incubated with different concentrations of PS-NH<sub>2</sub> (1, 5 and 50 μg/ml) and  
269 the results are reported in Fig. 2. As shown in Fig. 2A, a dose dependent decrease in LMS was  
270 observed (-50% at the highest concentration tested; p<0.05). Incubation with PS-NH<sub>2</sub> for different  
271 periods of time induced significant lysozyme release (Fig. 2B). Interestingly, both 5 and 50 μg/ml  
272 induced a large lysozyme release immediately after addition (up to +150% with respect to controls  
273 with the highest concentration; p<0.05), whereas after 30 min incubation a comparable increase was  
274 observed at all the concentrations tested (about +100%; p<0.05). On the other hand, no effect was  
275 observed at longer incubation times.

276



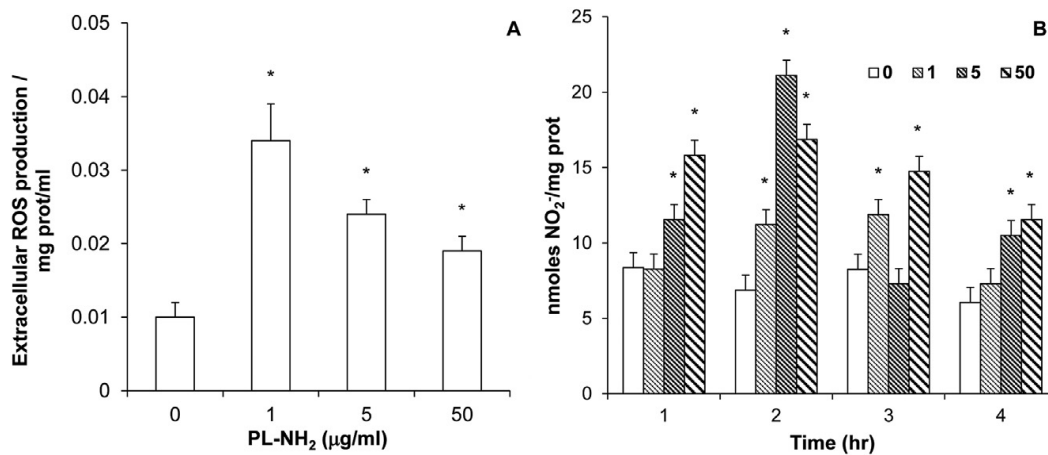
277  
278

279 Fig. 2. Effects of PS-NH<sub>2</sub> (1, 5, 50 μg/ml) on mussel hemocytes: A) Lysosomal membrane stability-LMS; B)  
280 extracellular lysozyme release, evaluated at different times of incubation (30 and 60 min). Data, representing the mean  
281 ± SD of four experiments in triplicate, were analysed by ANOVA followed by Tukey's post hoc test. Significant  
282 differences with respect to controls (p < 0.05) are reported (\*).  
283

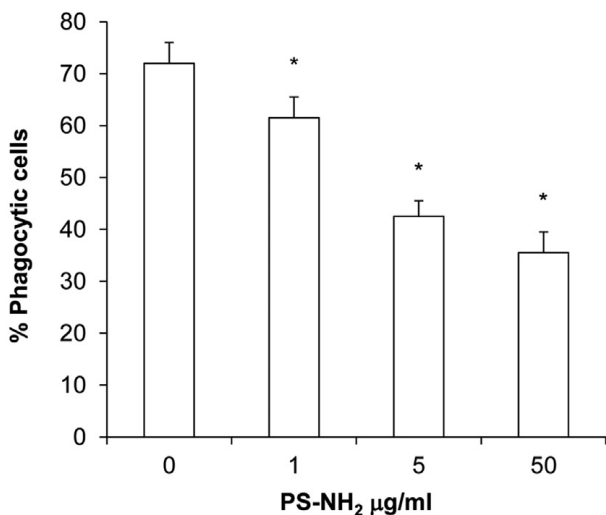
284 PS-NH<sub>2</sub> stimulated total extracellular oxyradical (or reactive oxygen species-ROS) production,  
285 evaluated as cytochrome *c* reduction at all the concentrations tested, with the highest increase



286 observed at the lowest concentration (about three-folds with respect to controls,  $p < 0.05$ ) (Fig 3A).  
 287 Nitric oxide-NO production was evaluated as nitrite accumulation in hemocytes incubated with PS-  
 288  $\text{NH}_2$  for different periods of time (from 1 to 4 h) (Fig. 3B). Significant increases were observed at  
 289 different concentrations, with the highest concentration stimulating NO production at all times of  
 290 exposure. However, the strongest effects were observed at 2 h incubation, with 5  $\mu\text{g}/\text{ml}$  eliciting the  
 291 highest response. Finally, PS- $\text{NH}_2$  induced a dose dependent decrease in phagocytosis, that was  
 292 significant from 1  $\mu\text{g}/\text{ml}$  and maximal at 50  $\mu\text{g}/\text{ml}$  (-16 and -50%, respectively;  $p < 0.05$ ) (Fig. 4).  
 293



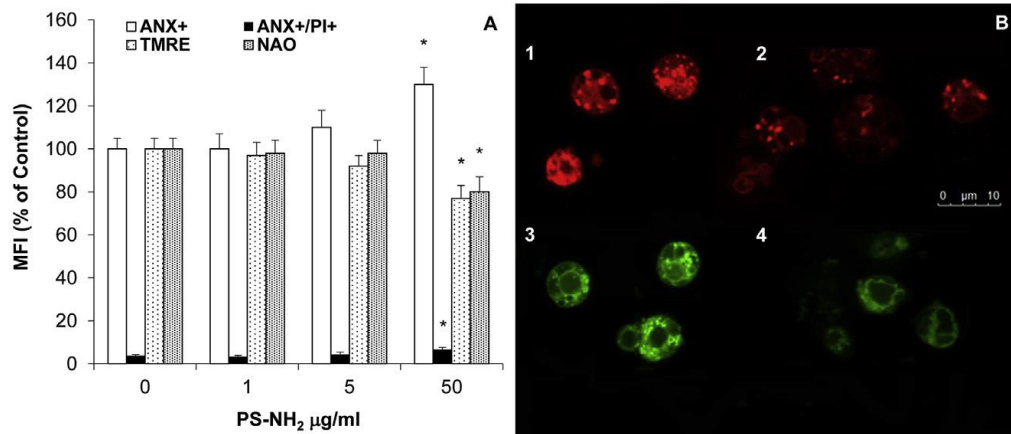
294  
 295  
 296 Fig. 3. Effects PS-NH<sub>2</sub> (1, 5, 50 mg/ml) on oxyradical and NO production by mussel hemocytes. A) extracellular  
 297 oxyradical production, evaluated as cytochrome c reduction in control  
 298 hemocytes and hemocytes exposed to PS-NH<sub>2</sub> for 30 min: B) NO production, evaluated as nitrite accumulation by the  
 299 Griess reaction, evaluated in control and PS-NH<sub>2</sub>-exposed hemocytes at different times of incubation (from 1 to 4 h).  
 300 Data, representing the mean  $\pm$  SD of four experiments in triplicate, were analysed by ANOVA followed by Tukey's post  
 301 hoc test. Significant differences with respect to controls ( $p < 0.05$ ) are reported (\*).  
 302



303  
 304  
 305 Fig. 4. Effects PS-NH<sub>2</sub> (1, 5, 50 mg/ml) on phagocytic activity of mussel hemocytes, evaluated as uptake of  
 306 Neutral-Red conjugated zymosan particles. Data, expressed as percentage of phagocytic cells and representing the mean  
 307  $\pm$  SD of four experiments in triplicate, were analysed by ANOVA followed by Tukey's post hoc test. Significant  
 308 differences with respect to controls ( $p < 0.05$ ) are reported (\*).  
 309

310 *3.3 Effects on apoptotic parameters*

311 The effects of PS-NH<sub>2</sub> incubation (45 min) on apoptotic parameters at both plasma membrane  
 312 and mitochondrial level were evaluated by Flow Cytometry utilizing specific fluorescent dyes for  
 313 phosphatidylserine externalization (Annexin V binding), mitochondrial membrane potential  $\Delta\psi_m$   
 314 (Tetramethylrhodamine, ethyl ester perchlorate-TMRE) and cardiolipin peroxidation in the inner  
 315 mitochondrial membrane (10-nonyl-acridine orange-NAO), and the results are reported in Fig. 5. A  
 316 significant increase in Annexin V positive-hemocytetes was induced by the highest concentration  
 317 tested (+30% with respect to control;  $p < 0.05$ ) (Fig. 5A). A small but significant increase in the  
 318 percentage of Annexin V/PI positive cells, indicating necrotic processes, was also observed. At 50  
 319  $\mu\text{g/ml}$ , significant decreases in TMRE fluorescence indicated decreases in mitochondrial membrane  
 320 potential  $\Delta\psi_m$  (-23% with respect to control;  $p < 0.05$ ); moreover, decreased NAO fluorescence  
 321 indicated cardiolipin peroxidation in the inner mitochondrial membrane (-20%;  $p < 0.05$ ). Such  
 322 decreases in fluorescence could not be easily appreciated by microscopical observations; however,  
 323 when cells were exposed to higher PS-NH<sub>2</sub> concentrations (100  $\mu\text{g/ml}$ ), larger decreases in both  
 324 TMRE and NAO fluorescence were observed, as shown by representative images obtained by  
 325 confocal microscopy (Fig. 5B).  
 326

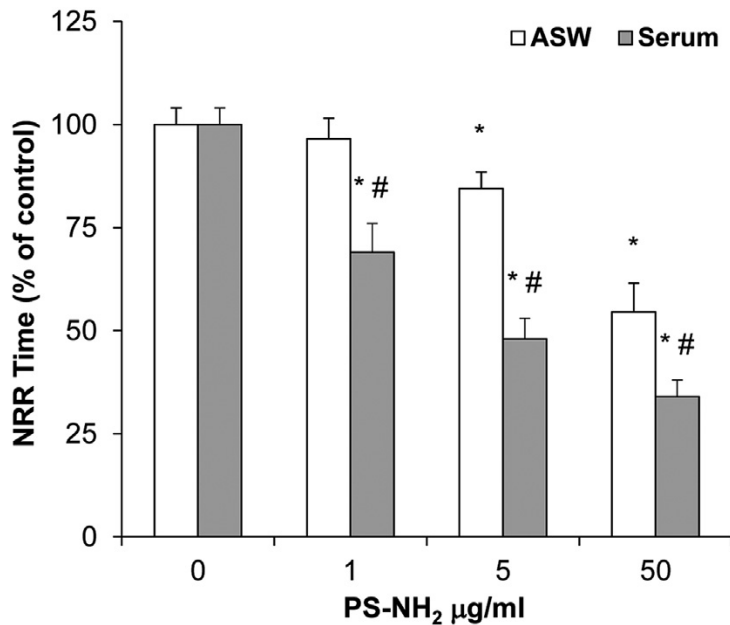


327  
 328  
 329 Fig. 5. Effect of PS-NH<sub>2</sub> on apoptotic parameters of mussel hemocytes. A) Flow cytometry: hemocytes were  
 330 exposed to PS-NH<sub>2</sub> (1, 5, 50 mg/ml) for 45 min, subsequently loaded with different fluorescent dyes and analysed as  
 331 described in Methods. Percentage of hemocytes positive to FITC Annexin V binding (ANX<sub>p</sub>) and to both ANX and PI  
 332 staining (ANX<sub>p</sub>/PI<sub>p</sub>) are reported. For mitochondrial parameters, cells were loaded with TMRE (for membrane  
 333 potential  $\Delta\psi_m$ ) and with NAO for cardiolipin content. Data are reported as Mean Fluorescence Intensities (MFI) (%  
 334 with respect to controls). Data, representing the mean  $\pm$  SD of three experiments, were analysed by ANOVA followed  
 335 by Tukey's post hoc test.  
 336 Significant differences with respect to controls ( $p < 0.05$ ) are reported (\*). B) Confocal fluorescence microscopy:  
 337 representative confocal images of hemocytes exposed in the same experimental conditions to PS-NH<sub>2</sub> (100 mg/ml) and  
 338 loaded with TMRE or NAO for determination of mitochondrial parameters. 1e2: TMRE (543 excitation/633 emission  
 339 filter set, red); 3e4: NAO (518 excitation/530 emission filter set, green) (60x magnification). 1: Control TMRE; 2: PS-  
 340 NH<sub>2</sub> TMRE; 3: Control NAO; 4: PS-NH<sub>2</sub> NAO. A decrease in both TMRE and NAO fluorescence can be appreciated  
 341 in cells exposed to PS-NH<sub>2</sub> compared to untreated cells. (For interpretation of the references to color in this figure  
 342 legend, the reader is referred to the web version of this article.)  
 343

#### 344 3.4. Effects of hemolymph serum on PS-NH<sub>2</sub>-induced lysosomal damage

345  
 346 Hemocyte LMS was also evaluated in samples incubated for 30 min with PS-NH<sub>2</sub> in the  
 347 presence hemolymph serum (1, 5, 50  $\mu\text{g/ml}$ ), and the results were compared with those obtained in  
 348 ASW. As shown in Fig. 6, a clear dose-dependent decrease in LMS was clearly observed (-32, -51  
 349 and -66% respectively;  $p < 0.05$ ). Such an effect was stronger than that observed in ASW at all the

350 concentrations tested, indicating that the hemolymph soluble fraction significantly increased  
351 lysosomal damage induced by PS-NH<sub>2</sub>.  
352



353  
354  
355 Fig. 6. Effects of hemolymph serum on PS-NH<sub>2</sub> e induced lysosomal membrane destabilization in mussel  
356 hemocytes. Cells were incubated as described in methods with PS-NH<sub>2</sub> suspensions (1, 5, 50 mg/ml) in either ASW or  
357 in hemolymph serum. Data, representing the mean ± SD of four experiments in triplicate, were analysed by ANOVA  
358 followed by Tukey's post hoc test (p < 0.05). \* all treatments vs controls; # serum vs ASW.  
359

#### 360 4. Discussion

361 In mammalian cells, the adverse effects of NPs, including nanoplastics, are commonly  
362 observed through measuring different physiological endpoints, including those related to lysosomal  
363 function, oxidative stress, inflammation, apoptosis (Bexiga et al., 2011; Lunov et al., 2011; Stern et  
364 al., 2012; Wang et al., 2013; Fleischer and Payne, 2014). In this work, a battery of functional assays  
365 was applied to investigate the possible effects of PS-NH<sub>2</sub> in the immune cells, the hemocytes, of the  
366 marine bivalve *M. galloprovincialis*.

367 With regards to characterization of PS-NH<sub>2</sub> suspensions, the low aggregation shown by PS-  
368 NH<sub>2</sub> in ASW (Figure 1) is still slightly higher compared to what observed in natural sea water and  
369 reported in our previous study (Della Torre et al., 2014). Further, the measured ζ-potential as +14.2  
370 mV resulted lower than that obtained in MilliQ water (+42.8 mV) (data not shown), indicating a  
371 screening effect of surface charges due to the higher salt content of ASW.

372 The results show that short term exposure (30 min) to PS-NH<sub>2</sub> induced rapid lysosomal  
373 destabilization at increasing concentrations. PS-NH<sub>2</sub> were able to stimulate lysosomal enzyme  
374 release, evaluated as extracellular lysozyme activity, also at concentrations as low as 1 µg/ml, with  
375 maximal effects at 30 min at all the concentrations tested. PS-NH<sub>2</sub> also induced extracellular  
376 oxyradical production, as well as NO production, with significant effects at lower concentrations (1-  
377 5 µg/ml). Finally, a dose dependent decrease in phagocytic activity was also observed. Overall, the  
378 results indicate that lower concentrations of PS-NH<sub>2</sub> elicited the release of hydrolytic enzymes and  
379 oxygen and nitrogen based reactive species, which represents the first inflammatory response  
380 induced by non-self material. On the other hand, at higher concentrations (50 µg/ml), a dramatic

381 decrease in phagocytosis and strong lysosomal destabilization were observed, indicating  
382 impairment of immunocompetence and lysosomal damage. These data were supported by the  
383 results obtained on apoptotic parameters evaluated by flow cytometry. At 50  $\mu\text{g/ml}$  PS-NH<sub>2</sub>  
384 induced significant increases in Annexin V staining, indicating phosphatidylserine externalization at  
385 the plasma membrane, as well as decreases in mitochondrial membrane potential and increased  
386 cardiolipin peroxidation in the inner mitochondrial membrane; all these effects were detected as  
387 early as 45 min of exposure. Interestingly, further increasing PS-NH<sub>2</sub> concentration (up 100  $\mu\text{g/ml}$ )  
388 resulted in larger decreases in both TMRE and NAO fluorescence (about 60% and 40%,  
389 respectively; not shown) that could be easily appreciated by confocal microscopy. Pre-apoptotic  
390 signs at mitochondrial level were previously observed in hemocytes exposed to nanosized carbon  
391 black (NCB) (Canesi et al., 2008) and ZnO NPs (Ciacci et al., 2012). In contrast, in human cells,  
392 PS-NH<sub>2</sub> induced lysosomal damage at longer times of incubation (within 3-6 h of exposure),  
393 whereas phosphatidylserine exposure and loss of mitochondrial membrane potential could be  
394 detected after 6-8 h exposure (Wang et al., 2013). From these data obtained in human cells, a  
395 description of the evolution of apoptotic cell death in which lysosomal damage plays a central role  
396 has been hypothesized for PS-NH<sub>2</sub> (Wang et al., 2013). This could also apply to the cells of marine  
397 invertebrates; actually, the first indication of interactions of NPs with bivalve cells was the  
398 observation of endosomal and lysosomal accumulation and oxyradical production following  
399 endocytosis of Nile red labeled sucrose polyester nanoparticles in isolated *Mytilus* digestive gland  
400 cells (Moore, 2006). Induction of apoptotic pathways has been also observed in the sea urchin  
401 embryo exposed to PS-NH<sub>2</sub> at 24 h post fertilization (Della Torre et al., 2014). Moreover, our  
402 results, indicating common mechanisms of action of PS-NH<sub>2</sub> in *Mytilus* hemocytes and human  
403 cells, suggest that similar pathways may be activated in the cells of marine invertebrates. In mussel  
404 hemocytes, functional responses as well as cellular damage and induction of apoptotic processes  
405 were particularly rapid, occurring within 1 h of exposure. This is in line with the physiological role  
406 of hemocytes, which are responsible for cell mediated immunity and represent the first line of  
407 defence against non self material in bivalves (Canesi et al., 2002; Canesi and Procházková, 2013).

408 The evaluation of the biological effects of NPs requires a molecular-level understanding of  
409 how NPs interact with cells in a physiological environment. In mammalian systems, extracellular  
410 serum proteins adsorb onto the NP surface, forming a protein “corona” (Lundquist et al., 2008;  
411 Fleischer and Payne, 2014 and refs. quoted therein). The protein corona formed by both PS-NH<sub>2</sub>  
412 and PS-COOH has been recently investigated in detail, underlying the role of albumin (BSA), the  
413 major serum protein (Fleischer and Payne, 2014). The results obtained in this work showed that the  
414 presence of hemolymph serum significantly increased the lysosomal damage induced by PS-NH<sub>2</sub> in  
415 the hemocytes, with significant effects at concentrations as low as 1  $\mu\text{g/ml}$ . These data, although  
416 preliminary, underline how also in *Mytilus* soluble serum components can affect NP interactions  
417 with cells, and suggest that a NP-protein corona might also be formed in biological fluids of marine  
418 invertebrates. This possibility is intriguing, since the corona proteins control the specific cellular  
419 receptors used by protein-NP complex, the cellular internalization pathways, and the immune  
420 response (Fleischer and Payne, 2014 and refs. quoted therein). Soluble hemolymph components of  
421 *Mytilus* hemolymph have been recently characterized (Oliveri et al., 2014), demonstrating that the  
422 Extrapallial Protein (EP) precursor, or putative C1q domain containing protein MgC1q6, represents  
423 the most abundant serum protein in mussels. Since understanding the protein corona is crucial for  
424 understanding how NPs interact with cells *in vivo*, interactions of NPs, including PS-NH<sub>2</sub>, with

425 hemolymph serum proteins deserve further investigation.

426 Acute ecotoxicity of cationic PS-NPs was assessed on a test battery of freshwater organisms  
427 representing different trophic levels (Casado et al., 2013). However, toxic effects were observed at  
428 high concentration, where high agglomeration and sedimentation of NPs were observed, this  
429 underlying the unsuitability of classical ecotoxicity tests for NP assessment. Apart from traditional  
430 ecotoxicity testing, it has been underlined how more specific assays, like immunotoxicity tests, may  
431 help understanding the major toxic mechanisms and modes of action that could be relevant for  
432 different nanomaterials in different organisms (Crane et al., 2008). Cell-mediated immunity and the  
433 phagocytic cells are being identified as the primary target of NPs in aquatic organisms (Jovanovic  
434 and Palic, 2012). The results obtained in mussel hemocytes represent the first data on the effects  
435 and mechanisms of action of nanoplastics at a cellular level in marine organisms. Overall, the  
436 results demonstrate that in *Mytilus* hemocytes PS-NH<sub>2</sub> elicited rapid effects also at low  
437 concentrations, with mechanisms similar to those observed in mammalian cells. The application of  
438 a battery of functional tests on *Mytilus* hemocytes has been proven as a powerful tool for the rapid  
439 screening of the immunomodulatory effects of different types of NPs in cell models of marine  
440 organisms, as well as robust alternative methods for testing the toxicity of NPs and a possible basis  
441 for designing of environmentally safer nanomaterials (reviewed in Canesi et al., 2012; Canesi and  
442 Procházková, 2013). This may also apply to nanoplastics and may help understanding their possible  
443 impact in the marine environment.

444 Despite many studies have described the increasing occurrence of microplastic in the marine  
445 environment (Andrady et al., 2011; Cole et al., 2011; Hidalgo-Ruz et al., 2012, Wright et al., 2012),  
446 much less is known about their degradation into smaller particles and no data on nanoplastic  
447 concentrations in environmental samples are available yet. However, nanoplastics may become a  
448 threat in the future for marine organisms when the large amount of microplastic decays, and with  
449 the rapidly increasing industrial production of NPs, including nanoplastics, for all kinds of  
450 applications (Wegner et al., 2012), with predicted concentrations for most nano materials higher  
451 than in 2009 (Sun et al., 2014). Moreover, sorption of other chemical pollutants to nanoplastics,  
452 like to other NPs, may affect their biological impact (Canesi et al., 2015). In this light, further  
453 studies are needed to investigate the potential effects of nanoplastics on marine organisms.

454

#### 455 **Acknowledgments**

456 PS NPs secondary characterisation was performed by Second Level degree student Elisa  
457 Bergami at the Centre for BioNano Interactions (University College of Dublin) funded by the  
458 Erasmus Long Life Learning Programme (year 2012–2013).

459

460

461 **References**

- 462
- 463 ASTM, 2004. International Standard guide for conducting static acute toxicity tests starting with  
464 embryos of four species of salt water bivalve mollusks. E 724-98.
- 465 Andradý, A.L., 2011. Microplastics in the marine environment. *Mar. Pollut. Bull.* 62, 1596-1605.
- 466 Bexiga, M.G., Varela, J.A., Wang, F., Fenaroli, F., Salvati, A., Lynch, I., Simpson, J.C., Dawson,  
467 K.A., 2011. Cationic nanoparticles induce caspase 3-, 7- and 9-mediated cytotoxicity in a  
468 human astrocytoma cell line. *Nanotoxicology* 5, 557-567.
- 469 Browne, M.A., Dissanayake, A., Galloway, T.S., Lowe, D.M., Thompson, R.C., 2008. Ingested  
470 microscopic plastic translocates to the circulatory system of the mussel, *Mytilus edulis* (L.).  
471 *Environ. Sci. Technol.* 42, 5026-5031.
- 472 Canesi, L., Gavioli, M., Pruzzo, C., Gallo, G., 2002. Bacteria - hemocyte interactions and  
473 phagocytosis in marine bivalves. *Microsc. Res. Techniq.* 57, 469-476.
- 474 Canesi, L., Ciacci, C., Betti, M., Fabbri, R., Canonico, B., Fantinati, A., Marcomini, A., Pojana, G.,  
475 2008. Immunotoxicity of carbon black nanoparticles to blue mussel hemocytes. *Environ. Int.*  
476 34, 1114-1119.
- 477 Canesi, L., Ciacci, C., Vallotto, D., Gallo, G., Marcomini, A., Pojana, G., 2010. In vitro effects of  
478 suspensions of selected nanoparticles (C60 fullerene, TiO<sub>2</sub>, SiO<sub>2</sub>) on *Mytilus* hemocytes. *Aq.*  
479 *Toxicol.* 96, 151-158.
- 480 Canesi, L., Ciacci, C., Fabbri, R., Marcomini, A., Pojana, G., Gallo, G., 2012. Bivalve molluscs as a  
481 unique target group for nanoparticle toxicity. *Mar. Environ. Res.* 76, 16-21.
- 482 Canesi, L., Procházková, P., 2013. The invertebrate immune system as a model for investigating the  
483 environmental impact of nanoparticles, in: Boraschi, D., Duschl, A. (Eds.), *Nanoparticles and*  
484 *the immune system*. Acad. Press, Oxford, pp. 91-112.
- 485 Canesi L, Ciacci C, Balbi T. 2015 Interactive effects of nanoparticles with other contaminants in  
486 aquatic organisms: Friend or foe? *Mar. Environ. Res.* doi: 10.1016/j.marenvres.2015.03.010
- 487 Casado, M. P., Macken, A., Byrne, H. J., 2013. Ecotoxicological assessment of silica  
488 and polystyrene nanoparticles assessed by a multitrophic test battery. *Environ. Int.* 51, 97-105.
- 489 Ciacci, C., Canonico, B., Bilaničová, D., Fabbri, R., Cortese, K., Gallo, G., Marcomini, A., Pojana,  
490 G., Canesi, L., 2012. Immunomodulation by different types of n-oxides in the hemocytes of the  
491 marine bivalve *Mytilus galloprovincialis*. *PLoS One* 7, e36937.
- 492 Cole, M., Lindeque, P., Halsband, C., Galloway, T.S., 2011. Microplastics as contaminants in the  
493 marine environment: A review. *Mar. Pollut. Bull.* 62, 2588–2597.
- 494 Corsi, I., Cherr, G.N., Lenihan, H.S., Labille, J., Hasselov, M., Canesi, L., Dondero, F., Frenzilli,  
495 G., Hristozov, D., Puntès, V., Della Torre, C., Pinsino, A., Libralato, G., Marcomini, A.,  
496 Sabbioni, E., Matranga, V., 2014. Common strategies and technologies for the ecosafety  
497 assessment and design of nanomaterials entering the marine environment. *ACS Nano* 8, 9694-  
498 9709.
- 499 Crane, M., Handy, R.D., Garrod, J., Owen, R., 2008. Ecotoxicity test methods and environmental  
500 hazard assessment for engineered nanoparticles. *Ecotoxicology* 17, 421-437.

- 501 Della Torre, C., Bergami, E., Salvati, A., Faleri, C., Cirino, P., Dawson, K.A., Corsi, I., 2014.  
502 Accumulation and embryotoxicity of polystyrene nanoparticles at early stage of development  
503 of sea urchin embryos *Paracentrotus lividus*. *Environ. Sci. Technol.* 48, 12302-12311.
- 504 Fleischer, C.C., Payne, C.K., 2014. Nanoparticle-cell interactions: molecular structure of the protein  
505 corona and cellular outcomes. *Acc. Chem. Res.* 47, 2651-2659.
- 506 Hidalgo-Ruz, V., Gutow, L., Thompson, R.C., Thiel, M., 2012. Microplastics in the marine  
507 environment: a Review of the methods used for identification and quantification. *Environ. Sci.*  
508 *Technol.* 46, 3060-3075.
- 509 Jovanovic, B., Palic, D., 2012. Immunotoxicology of non-functionalized engineered nanoparticles  
510 in aquatic organisms with special emphasis on fish-review of current knowledge, gap  
511 identification, and call for further research. *Aquat. Toxicol.* 15, 118-119.
- 512 Liu, Y.X., Li, W., Lao, F., Liu, Y., Wang, L.M., Bai, R., 2011. Intracellular dynamics of cationic  
513 and anionic polystyrene nanoparticles without direct interaction with mitotic spindle and  
514 chromosomes. *Biomaterials* 32, 8291-8303.
- 515 Lundqvist, M., Stigler, J., Elia, G., Lynch, I., Cedervall, T., Dawson, K. A. 2008. Nanoparticle size  
516 and surface properties determine the protein corona with possible implications for biological  
517 impacts. *Proc.Natl. Acad. Sci. U.S.A.* 105, 14265-14270.
- 518 Lunov, O., Syrovets, T., Loos, C., Nienhaus, U., Mailänder, V., Landfester, K., Rouis, M., Simmet,  
519 T., 2011. Amino-functionalized polystyrene nanoparticles activate the NLRP3 inflammasome  
520 in human macrophages *ACS Nano* 5, 9648-9657.
- 521 Matranga, V., Corsi, I., 2012. Toxic effects of engineered nanoparticles in the marine environment:  
522 model organisms and molecular approaches. *Mar. Environ. Res.* 76, 32-40.
- 523 Moore, M.N., 2006. Do nanoparticles present ecotoxicological risks for the health of the aquatic  
524 environment? *Environment International* 32, 967-976.
- 525 Nel, A.E., Madler, L., Velegol, D, Xia, T., Hoek, E.M.V., Somasundaran, P. 2009. Understanding  
526 biophysicochemical interactions at the nano-bio interface. *Nat. Mater.* 8:543-57.
- 527 Oliveri, C., Peric, L., Sforzini, S., Banni, M., Viarengo, A., Cavaletto, M., and Marsano, F. , 2014.  
528 Biochemical and proteomic characterisation of haemolymph serum reveals the origin of the  
529 alkali-labile phosphate (ALP) in mussel (*Mytilus galloprovincialis*). *Comp Biochem Physiol*  
530 *Part D Genomics Proteomics.* 11, 29-36.
- 531 PlasticsEurope, 2013. Plastics – the Facts 2013: an analysis of European latest plastics production,  
532 demand and waste data. <http://www.plasticseurope.org/Document/plastics-the-facts-2013.aspx>
- 533 Van Cauwenberghe L., Janssen, C.R., 2014. Microplastics in bivalves cultured for human  
534 consumption. *Environ. Poll.* 193, 65-70.
- 535 Sun, T.Y., Gottschalk, F., Hungerbühler, K., Nowack, B., 2014. Comprehensive probabilistic  
536 modelling of environmental emissions of engineered nanomaterials. *Environ Pollut.* 185, 69-76.
- 537 Stern, S.T., Adiseshiah, P.P., Crist, R.M., 2012. Autophagy and lysosomal dysfunction as  
538 emerging mechanisms of nanomaterial toxicity. *Part. Fibre Toxicol.* 9, 20.
- 539 Wang, F., Bexiga, M.G., Anguissola, S., Boya, P., Simpson, J.C., Salvati, A., Dawson, K.A., 2013.  
540 Time resolved study of cell death mechanisms induced by amine-modified polystyrene  
541 nanoparticles. *Nanoscale* 5, 10868-10876.

- 542 Ward, J.E.; Kach, D., 2009. Marine aggregates facilitate ingestion of nanoparticles by suspension-  
543 feeding bivalves. *Mar. Environ. Res.* 68, 137-142.
- 544 Wegner, A., Besseling, E., Foekema, E.M., Kamermans, P., Koelmans, A., 2012. A. Effects of  
545 nanopolystyrene on the feeding behavior of the blue mussel (*Mytilus edulis* L.). *Environ.*  
546 *Toxicol. Chem.* 31, 2490–2497.
- 547 Wright S.L., Thompson R.C., Galloway, T.S., 2013. The physical impacts of microplastics on  
548 marine organisms: A review. *Environ. Poll.* 178, 483-492.
- 549



550 **Legend to Figures**

551

552 Fig. 1 – Primary and secondary characterization of PS-NH<sub>2</sub> using TEM imaging and DLS,  
553 respectively. Left: TEM image of primary 50 nm PS-NH<sub>2</sub>. Scale bar: 200 nm. Right: Size  
554 distribution graph by intensity for PS-NH<sub>2</sub> suspension at 50 µg/ml in ASW, determined by Contin  
555 analysis (DLS Analysis). Three independent replicates are shown, the x-axis minimum set at 10 nm  
556 and a logarithmic scale is used for y-axis. The graph was edited using GraphPad Prism5.

557

558 Fig. 2 – Effects of PS-NH<sub>2</sub> (1, 5, 50 µg/ml) on mussel hemocytes: A) Lysosomal membrane  
559 stability-LMS; B) extracellular lysozyme release, evaluated at different times of incubation (30 and  
560 60 min). Data, representing the mean±SD of four experiments in triplicate, were analysed by  
561 ANOVA followed by Tukey's post hoc test. Significant differences with respect to controls  
562 (p≤0.05) are reported (\*).

563

564 Fig. 3 - Effects PS-NH<sub>2</sub> (1, 5, 50 µg/ml) on oxyradical and NO production by mussel hemocytes. A)  
565 extracellular oxyradical production, evaluated as cytochrome *c* reduction in control hemocytes and  
566 hemocytes exposed to PS-NH<sub>2</sub> for 30 min: B) NO production, evaluated as nitrite accumulation by  
567 the Griess reaction, evaluated in control and PS-NH<sub>2</sub>-exposed hemocytes at different times of  
568 incubation (from 1 to 4 hrs). Data, representing the mean±SD of four experiments in triplicate, were  
569 analysed by ANOVA followed by Tukey's post hoc test. Significant differences with respect to  
570 controls (p <0.05) are reported (\*).

571

572 Fig. 4 - Effects PS-NH<sub>2</sub> (1, 5, 50 µg/ml) on phagocytic activity of mussel hemocytes, evaluated as  
573 uptake of Neutral-Red conjugated zymosan particles. Data, expressed as percentage of phagocytic  
574 cells and representing the mean±SD of four experiments in triplicate, were analysed by ANOVA  
575 followed by Tukey's post hoc test. Significant differences with respect to controls (p <0.05) are  
576 reported (\*).

577

578 Fig. 5 – Effect of PS-NH<sub>2</sub> on apoptotic parameters of mussel hemocytes.

579 A) Flow cytometry : hemocytes were exposed to PS-NH<sub>2</sub> (1, 5, 50 µg/ml) for 45 min, subsequently  
580 loaded with different fluorescent dyes and analysed as described in Methods. Percentage of  
581 hemocytes positive to FITC Annexin V binding (ANX+) and to both ANX and PI staining  
582 (ANX+/PI+) are reported. For mitochondrial parameters, cells were loaded with TMRE (for  
583 membrane potential Δψ<sub>m</sub>) and with NAO for cardiolipin content. Data are reported as Mean  
584 Fluorescence Intensities (MIF) (% with respect to controls). Data, representing the mean±SD of  
585 three experiments, were analysed by ANOVA followed by Tukey's post hoc test. Significant  
586 differences with respect to controls (p <0.05) are reported (\*).

587 B) Confocal fluorescence microscopy: representative confocal images of hemocytes exposed in the  
588 same experimental conditions to PS-NH<sub>2</sub> (100 µg/ml) and loaded with TMRE or NAO for  
589 determination of mitochondrial parameters. 1-2: TMRE (543 excitation/633 emission filter set, red);  
590 3-4: NAO (518 excitation/530 emission filter set, green) (60x magnification).

591 1: Control TMRE; 2: PS-NH<sub>2</sub> TMRE; 3: Control NAO; 4: PS-NH<sub>2</sub> NAO. A decrease in both TMRE  
592 and NAO fluorescence can be appreciated in cells exposed to PS-NH<sub>2</sub> compared to untreated cells.

593

594 Fig. 6 – Effects of hemolymph serum on PS-NH<sub>2</sub> - induced lysosomal membrane destabilization in  
595 mussel hemocytes. Cells were incubated as described in methods with PS-NH<sub>2</sub> suspensions (1, 5, 50  
596 μg/ml) in either ASW or in hemolymph serum. Data, representing the mean±SD of four  
597 experiments in triplicate, were analysed by ANOVA followed by Tukey's post hoc test (p≤0.05).  
598 \* = all treatments vs controls; # = serum vs ASW.